Micellar Growth, Network Formation, and Criticality in Aqueous Solutions of the Nonionic Surfactant $C_{12}E_5$

A. Bernheim-Groswasser,† E. Wachtel,‡ and Y. Talmon*,†

Department of Chemical Engineering, Technion-Israel Institute of Technology, Haifa 32000, Israel and Chemical Services Unit, Weizmann Institute of Science, Rehovot 76100, Israel

Received September 17, 1999. In Final Form: February 1, 2000

We used cryo-TEM and light scattering to study the micellar growth and subsequent network formation in aqueous solutions of the nonionic surfactant $C_{12}E_5$. Cryo-TEM shows the first direct evidence for the existence of connected topology in the vicinity of the critical point and the two-phase separation curve of the $C_{12}E_5$/water micellar system. The coexisting phases within the two-phase region consist of one concentrated and one dilute network of interconnected cylindrical micelles. These findings are consistent with the recent theoretical explanation of criticality and phase separation in certain nonionic surfactant systems as resulting from entropic attraction between network junctions. Away from the two-phase separation curve, we have identified uniaxial micellar growth, with increasing temperature and concentration, into long threadlike micelles. From the power-law dependence of the radius of gyration, $R_{G,z}$, and the hydrodynamic diameter, $\bar{D}_H$, on the molecular weight ($R_{G,z}$, $\bar{D}_H \sim M_w^{\nu}$), we find that these threadlike micelles have properties resembling those of flexible polymers in a good solvent ($\nu \sim 0.6$). Static and dynamic light scattering show that the mean micelle contour length $\bar{L}$ increases as $c^{0.5}$ (c is the surfactant concentration) in agreement with theory. Finally, we show that the end-cap energy E_c increases linearly with temperature.

Introduction

An unresolved controversy concerns the relation between micellar growth, phase separation, and criticality in binary nonionic micellar systems. The phase separation and criticality have been the subject of many experimental and theoretical works. In the past, they were explained as resulting from interactions between small globular micelles[1,2] or due to increasing attraction between growing micelles.[3−5] Recently, Tlusty et al.[6] suggested that network entropy alone can give rise to phase separation and criticality in nonionic microemulsions. That theory was recently supported experimentally by cryo-TEM observation of the $C_{12}E_5/H_2O/n$-octane system.[7] It was also proposed that the same arguments may be appropriate for the explanation of criticality and phase separation in certain binary nonionic micellar systems through the coexistence of concentrated and dilute networks of interconnected (branched) cylindrical micelles.[7] The present work shows by cryo-TEM the existence of micellar networks in the vicinity of the critical point and two-phase separation curve. These direct structural observations corroborate the relation between criticality and phase separation of binary systems and the existence of micellar networks.

Branched threadlike micelles can be formed in dilute or semidilute surfactant solutions depending on the magnitude of a control parameter such as temperature, concentration of added salt, or cosurfactant.[8] Indeed, unusual rheological behavior in the CTAB/KBr[9] and $CPClO_3/NaClO_3$ systems[9,10] was related to the formation of a multiconnected branched micellar network instead of a semidilute solution of entangled threadlike micelles. This supported the theories of Drye and Cates[11] and Bohbot et al.,[12] who had proposed the formation of networks of branched cylindrical micelles. It is difficult to find experimental evidence to support the existence of such branches. Scattering techniques (light and neutron) cannot distinguish between entangled and branched networks. The only available technique to unambiguously distinguish between branched and unbranched micelles is cryo-TEM.[7,13−15]

In this work, we studied dilute aqueous micellar solutions of the nonionic surfactant pentaoxyethylene glycol mono-*n*-dodecyl ether, denoted $C_{12}E_5$. The temperature has a crucial effect on the phase diagram of this system in general and on the microstructures of the micellar phase in particular.[16] For $c_c = 1.08$ wt % (c_c = critical surfactant concentration in weight percent), this system exhibits a critical temperature, $T_c = 31.5$ °C, above which the isotropic micellar phase (denoted by L_1) separates into two coexisting phases, poor (dilute; denoted

* To whom correspondence should be addressed.
† Technion-Israel Institute of Technology.
‡ Weizmann Institute of Science.

(1) Corti, M.; Degiorgio, V. *J. Phys. Chem.* **1981**, *85*, 1442.
(2) Corti, M.; Minero, C.; Degiorgio, V. *J. Phys. Chem.* **1984**, *88*, 309.
(3) Blankschtein, D.; Thurston, G. M.; Benedek, G. B. *J. Chem. Phys.* **1986**, *85*, 7268.
(4) Balmbra, R. R.; Clunie, J. S.; Corkill, J. M.; Goodman, J. F. *Trans. Faraday Soc.* **1962**, *58*, 1661.
(5) Balmbra, R. R.; Clunie, J. S.; Corkill, J. M.; Goodman, J. F. *Trans. Faraday Soc.* **1964**, *60*, 979.
(6) Tlusty, T.; Safran, S. A.; Menes, R.; Strey, R. *Phys. Rev. Lett.* **1997**, *78*, 2616.
(7) Bernheim-Groswasser, A.; Tlusty, T.; Safran, S. A.; Talmon, Y. *Langmuir* **1999**, *15*, 5448.
(8) Lequeux., F.; Candau, S. J. In *Structure and Flow in Surfactant Solutions*; Herb, C. A., Prud'homme, R. K., Eds.; ACS Symposium series 578; American Chemical Society: Washington, DC, 1994; p 51.
(9) Candau, S. J.; Khatory, A.; Lequeux, F.; Kern, F. J. *Physique IV* **1993**, *3*, 197.
(10) Appell, J.; Porte, G.; Khatory, A.; Kern, F.; Candau, S. J. *J. Phys. II* (*France*) **1992**, *2*, 1045.
(11) Drye, T. J.; Cates, M. E. *J. Phys. Chem.* **1992**, *96*, 1367.
(12) Bohbot, Y.; Ben-Shaul, A.; Granek, R.; Gelbart, W. M. *J. Chem. Phys.* **1995**, *103*, 8764.
(13) Danino, D.; Talmon, Y.; Levy, H.; Beinert, G.; Zana, R. *Science* **1995**, *269*, 1420.
(14) Oda, R.; Panizza, P.; Schmutz, M.; Lequeux, F. *Langmuir* **1997**, *13*, 6407.
(15) Lin, Z. *Langmuir* **1996**, *12*, 1729.
(16) Strey, R.; Schomacker, R.; Roux, D.; Nallet, F.; Olsson, U. *J. Chem. Soc., Faraday Trans.* **1990**, *86*, 2253.

10.1021/la991231q CCC: $19.00
Published on Web 04/06/2000

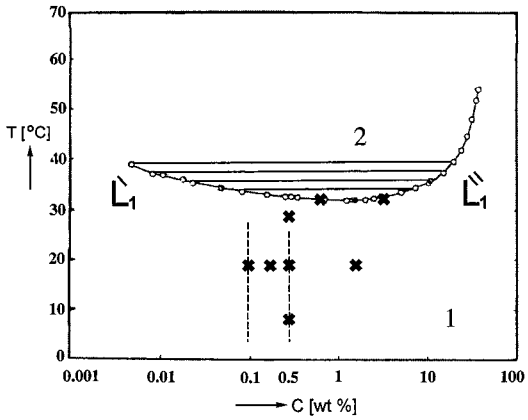

Figure 1. Schematic phase diagram and lower miscibility gap of the $C_{12}E_5$−water system (after ref 17). The dashed lines mark the region in the phase diagram in which light scattering experiments were conducted, and (×) marks the points where cryo-TEM images were taken.

by L_1') and rich (concentrated; denoted by L_1'') in surfactant (Figure 1).[17]

The effects of temperature and concentration on micelle size, shape, and growth in the $C_{12}E_5/H_2O$ system have been major issues in earlier studies. Self-diffusion NMR[18] and dynamic light scattering (DLS)[19,20] measurements carried out on dilute solutions showed that raising the temperature induces micellar growth. In addition, for higher surfactant concentrations, static (SLS) and dynamic (DLS) light scattering demonstrated that the micellar solutions resemble semidilute solutions of entangled flexible polymers.[21] Based on those observations, we have tried to determine whether this micellar growth is indeed one-dimensional (uniaxial) under very dilute conditions. Sufficient growth may lead to the formation of threadlike micelles having some flexibility and properties similar to polymer molecules in solution. The existence of polymer-like phases associated with the formation of long flexible cylinders by surfactant aggregation in aqueous solutions has been suggested by Porte et al.,[22] and has been extended to microemulsions by Safran et al.[23] Numerous experimental studies performed in the semidilute regime have reinforced the analogy between real polymers and polymer-like micelle solutions.[21,24−26] However, there is a major difference between polymer solutions and threadlike micellar systems. This difference is related to the self-aggregation nature of the formation of cylindrical micelles, which leads to equilibrium "polymers" with a broad distribution of micellar sizes.[26,27] According to theory, for neutral and screened ionic micelles the average contour length, $\bar{L}$, depends on surfactant concentration, c, as $c^{1/2}$, and exponentially on the ratio of the end-cap energy, E_c, and the temperature, as $E_c/2k_BT$.[26,27] In addition, their dynamics are quite different from polymer solutions, since the micelles spontaneously disassemble and reassemble in time.

We present here our studies of the effect of temperature and surfactant concentration on micellar topology in solutions of the $C_{12}E_5$/water binary system. We combined three complementary techniques: cryo-TEM, SLS, and DLS. SLS experiments provided information about the size of the micelles, whereas DLS gave information about hydrodynamic properties. Light scattering experiments were performed in the $C_{12}E_5$ concentration range of 0.1 to 0.5 wt % and in the temperature range of 8 to 28 °C, where the assumption of a dilute regime condition is valid.[21] Intermicellar interactions for such low surfactant concentrations are assumed to be negligible. Cryo-TEM provides direct indispensable qualitative information for the interpretation of the light scattering data. More importantly, cryo-TEM enables us to visualize micellar topology, branched network or disconnected cylinders, close to the critical temperature and the two-phase separation curve, and to assess the novel theory of phase separation and criticality for certain nonionic surfactants.[6]

Here, we report the first direct evidence by cryo-TEM imaging for the existence of networks in the proximity of the critical point and the two-phase separation curve. The coexisting phases within the two-phase region are concentrated and dilute networks of interconnected cylindrical micelles. Away from the two-phase separation curve, we have identified uniaxial micellar growth with increasing temperature and concentration into long threadlike micelles. These threadlike micelles were found to have properties resembling those of flexible polymers in a good solvent ($\nu \sim 0.6$). Static and dynamic light scattering show that the mean micelle contour length $\bar{L}$ increases as $c^{0.5}$ in agreement with theory. Finally, we show that the end-cap energy E_c increases linearly with temperature.

Experimental Section

Materials. The surfactant $C_{12}E_5$ was purchased from Nikko Chemical Co., Ltd. (Tokyo, Japan). It was stored in the dark at −20 °C and used without further purification. Solutions were prepared by adding Millipore water to weighed quantities of the surfactant.

Cryo-TEM. Specimens were prepared in a controlled environment vitrification system (CEVS),[28] at controlled temperature and relative humidity to avoid loss of water. A drop of solution was placed on a TEM grid covered by a holey carbon film. The drop was then blotted with a filter paper to form a thin liquid film on the grid, which was then immediately plunged into liquid ethane at its freezing temperature. The vitrified specimens were observed in a Philips CM120 transmission electron microscope at an accelerating voltage of 120 kV, at approximately −175 °C, in an Oxford Instruments CT3500 cryo-specimen holder. Images were digitally recorded by a Gatan MultiScan 791 CCD camera at about 4 μm underfocus to enhance phase-contrast.

Light Scattering. $C_{12}E_5$ solutions were first centrifuged for 2 h at 2000g to remove dust particles. Each solution was then transferred into a cylindrical scattering cell (diameter 2.9 cm) which was placed in a "vat" filled with toluene as the optical matching fluid. During the course of the measurements, the vat was kept at constant temperature (± 0.1 °C). The light source was an argon ion laser (Spectra Physics, λ = 514.5 nm), and photons scattered by the sample were collected by an ITT PW130 photomultiplier tube mounted on the goniometer arm at angles $45° < \theta < 135°$ to the direction of the incident beam.

(17) Strey, R. *Ber. Bunsen-Ges. Phys. Chem.* **1996**, *100*, 182.
(18) Nilsson, P. G.; Wennerström, H.; Lindman, B. *J. Phys. Chem.* **1983**, *87*, 1377.
(19) Martin, A.; Lesemann, M.; Belkoura, L.; Woermann, D. *J. Phys. Chem.* **1996**, *100*, 13760.
(20) Kato, T.; Anzai, S.; Takano, S.; Seimiya, T. *J. Chem. Soc., Faraday Trans. 1* **1989**, *85*, 2499.
(21) Kato, T.; Anzai, S.; Seimiya, T. *J. Phys. Chem.* **1990**, *94*, 7255.
(22) Appell, J.; Porte, G. *J. Phys. Lett.* **1983**, *44*, L-689. Porte, G.; Appell, J. In *Physics of Amphiphiles: Micelles, Vesicles and Microemulsions*; Degiorgio, V., Corti, M., Eds.; North-Holland Physics Publishing: Amsterdam, 1985; p 461.
(23) Safran, S. A.; Turkevitch, L A.; Pincus, P. *J. Physique Lett.* **1984**, *45*, L-69.
(24) Cabane, B.; Duplessix, R.; Zemb, Th. In *Surfactant in Solutions*; Lindman, B., Mittal, K., Eds.; Plenum Press: New York, 1984.
(25) Lin, Z.; Scriven, L. E.; Davis, H. T. *Langmuir* **1992**, *8*, 2200.
(26) Cates, M. E.; Candau, S. J. *J. Phys.: Condens. Matter* **1990**, *2*, 6869 and references therein.
(27) Israelachvili, J. N.; Mitchell, D. J.; Ninham, B. W. *J. Chem. Soc., Faraday Trans. 2* **1976**, *72*, 1525.
(28) Talmon, Y. In *Modern Characterization Methods of Surfactant Systems*; Binks, B. P., Ed.; Marcel Dekker: New York, 1999; p 147.

SLS. The intensity data were corrected for background (cell and water) scattering and converted into Rayleigh ratios (absolute scattered intensities), $R(q)$, using toluene as the reference standard. The Rayleigh ratio was calculated using

$$R(q) = \frac{\Delta\langle I(q)\rangle}{\langle I_{tol}\rangle} R_{tol}\left(\frac{n}{n_{tol}}\right)^2 \quad (1)$$

where $q = (4\pi n/\lambda_0)\sin(\theta/2)$ is the amplitude of the scattering wavevector, θ the scattering angle, and λ_0 the wavelength of the incident light in vacuum. $\Delta\langle I(q)\rangle = \langle I_{sol}(q)\rangle - \langle I_{back}(q)\rangle$ is the average scattered intensity of the solution after background subtraction, $\langle I_{tol}\rangle$ is the average scattered intensity of the toluene, $R_{tol} = 35.8 \times 10^{-4}$ m^{-1} is the Rayleigh ratio of toluene,[29] and n and n_{tol} are the index of refraction of solution and toluene, respectively.

DLS. The photoelectron count-time autocorrelation function was measured with a BI 2030AT (Brookhaven Instruments) digital autocorrelator and was analyzed using the constrained regularization algorithm, CONTIN.[30]

Theoretical Background. In dilute solution, micellar size can be probed by studying the scattering and hydrodynamic properties of the system.[31] The scattered light intensity is usually expressed in terms of $R(q)$:

$$R(q) = KcM_w P(q) S(q) \quad (2)$$

K is constant for a given system and is given by $4\pi^2 n^2 (\partial n/\partial c)^2 / N_A \lambda_0^4$, where n is the refractive index of the solution. $\partial n/\partial c$, the refractive index increment used here, is given by $0.1346 - (2.5e^{-4})(T - 25)$, where T is the temperature in °C.[32] N_A is Avogadro's number, M_w is the weight-average molecular weight in g/mol, and c is the concentration of $C_{12}E_5$ in mg/cm^3.[33] $P(q)$ is the form factor of the particle, and $S(q)$ is the structure factor. In dilute solutions, in the limit $q \to 0$, $P(q) \to 1$, eq 2 becomes

$$R(0) = KcM_w S(0) = KcM_w(1 - 2A_2M_w c + ...) = KcM_{w,app} \quad (3)$$

where A_2 is the second virial coefficient. M_w increases with concentration for surfactant systems as c^α, resulting in an increase in $R(0) \sim c^{1+\alpha}$. This is in contrast to semidilute solutions, for which it was previously shown that $R(0) \sim c^{-0.31}$.[34]

In the limit of low angles ($qR_G \ll 1$), $P(q)$ has a Lorentzian form and eq 2 becomes

$$\frac{Kc}{R(q)} = \frac{1}{M_{w,app}}\left[1 + \frac{(qR_{G,z})^2}{3}\right] \quad (4)$$

where $R_{G,z}$, the z-average micellar radius of gyration, and the apparent weight-average molecular weight, $M_{w,app}$, (see eq 3) are obtained from the slope and the intercept, respectively, when $Kc/R(q)$ is plotted versus q^2. The major problem encountered in an accurate determination of micellar molecular weight, M_w, arises from the effect of interactions which cannot be neglected for ionic surfactants (even at high dilution) and which strongly depends on the salt content. In the case of nonionic surfactants, although this problem still exists it is assumed to be minor at low enough concentrations. In "ordinary" polymers, this difficulty is overcome by extrapolating the experimental data to zero concentration. This procedure cannot be applied to the case of micellar solutions, since the molecular weight of the micelles is an increasing function of the surfactant concentration.

Hydrodynamic properties of the particles in solution can be characterized by DLS. With DLS, one measures the time autocorrelation function of the fluctuations in the light scattered from particles in solution:

$$g^{(2)}(q, t) = A + B(g^{(1)}(q, t))^2 \quad (5)$$

In eq 5, A is the baseline determined for the largest t when all correlation is lost, B is an optical constant of the system, and $g^{(1)}(q, t)$ for a polydisperse system is given by

$$g^{(1)}(q, t) = \int_0^\infty A(\Gamma) e^{-\Gamma t}\, d\Gamma \quad (6)$$

where Γ is a decay rate. The CONTIN method, developed by Provencher[30] for calculating the Laplace transform of $g^{(1)}(q, t)$, was used for the determination of Γ and $A(\Gamma)$. The function $A(\Gamma)$ is converted into an intensity-weighted distribution of the mutual translational diffusion coefficients, D, of the scattering particles, which is defined as $\Gamma/q^2 \to D$ when $q \to 0$. The resulting unimodal distribution is characterized by the z-average diffusion coefficient, $\bar{D}_z$. The average hydrodynamic diameter, $\bar{D}_H$, is related to $\bar{D}_z$ by the Stokes−Einstein relation:[35]

$$\bar{D}_H = \frac{k_B T}{6\pi\eta_0 \bar{D}_z} \quad (7)$$

where T is the absolute temperature, k_B is the Boltzmann constant, and η_0 is the viscosity of the solvent at temperature T.

In "real" polymer solutions, both the radius of gyration, R_G, and the hydrodynamic diameter, D_H, are related to the molecular weight by a simple power law:

$$D_H \sim M_w^{\nu} \text{ and } R_G \sim M_w^{\nu} \quad (8)$$

where ν is 0.5 and 0.588 for a θ solvent and a good solvent, respectively.[34,36] If a similar relation can be found for the micellar aqueous solution, this would reinforce the analogy already suggested between the micellar and polymer solutions.

Elongated micelles are locally cylindrical aggregates, with two smoothly connected spherical end-caps of radius larger than the cylinder core.[37−39] To find the dependence of the average contour length, $\bar{L}$, on c and T for cylindrical micelles, we use $M_{w,app}$ obtained from SLS measurements. $\bar{L}$ (weight average) is calculated assuming (1) a micelle is made of a cylindrical core of radius r_c with surfactant area per headgroup A_c; (2) the possible presence of branch points is neglected; and (3) values for the radius and area per headgroup are $r_c = 1.55$ nm, $A_c = 0.452$ nm^2.[40,41] The mean aggregation number of the micelles, N_{agg}, is equal to $M_{w,app}/M_o$, where M_o, the surfactant monomer molecular weight, is 406

(29) Moreels, E.; De Ceuninck, W.; Finsy, R. *J. Chem. Phys.* **1987**, *86*, 618.

(30) Provencher, S. *Comput. Phys. Commun.* **1982**, *27*, 229.

(31) Lang, J.; Zana, R. In *Surfactant in Solutions*; Zana, R., Ed.; Marcel Dekker: New York, 1987; p 405 and references therein.

(32) Richtering, W. H.; Burchard, W.; Jahns, E.; Finkelmann, H. *J. Phys. Chem.* **1988**, *92*, 6032.

(33) The critical micelle concentration (CMC) for $C_{12}E_5$ in water at 32 °C is 2.9×10^{-3} wt % (see Schubert, K.-V.; Strey, R.; Kahlweit, M. *J. Colloid Interface Sci.* **1991**, *141*, 21). This is much lower than the surfactant concentrations used here. The temperature dependence of the CMC is not available, but, for example, we were unable to detect excess scattering from such a binary mixture at 25 °C. Accordingly, the weighed-in values of surfactant were used to determine the relevant concentrations.

(34) de Gennes, P. G. *Scaling Concepts in Polymer Physics*; Cornell University Press: Ithaca, New York, 1976.

(35) Shurtenberger, P.; Mazer, N.; Känzig, W. *J. Phys. Chem.* **1983**, *87*, 308.

(36) Schaefer, D. W.; Joanny, J. F.; Pincus, P. *Macromolecules* **1980**, *13*, 1280.

(37) Danino, D.; Bernheim-Groswasser, A.; Talmon, Y. *Langmuir*, submitted for publication.

(38) Tlusty, T.; Safran, S. A. *J. Phys. Condens. Matter* **2000**, *12*, 1. These calculations were basically made for microemulsions and thus use the familiar Helfrich curvature energy expression (see Helfrich, W. Z. *Naturforsch.* **1973**, *28c*, 693) valid only for small curvature deformations, thus not valid for micelles. However, it was shown that this crude approximation provides a reasonable estimation of micelle properties; see May, S.; Bohbot, Y.; Ben-Shaul, A. *J. Phys. Chem. B* **1997**, *101*, 8648.

(39) Surfactant molecules residing in larger spherical end-caps can pack in lower curved surface, with smaller area per headgroup than if the two radii were equal, thus minimizing their packing free energy (see Bernheim-Groswasser, A.; Zana, R.; Talmon, Y. and references therein; *J. Phys. Chem. B*, in press.

(40) Medhage, B.; Mats, A.; Jan, A. *J. Phys. Chem.* **1993**, *97*, 7753.

(41) Glatter, O.; Strey, R.; Schubert, K. V.; Kaler, E. W. *Ber. Bunsen-Ges. Phys. Chem.* **1996**, *100*, 323.

g/mol. $\bar{L}$ is then given by

$$\bar{L} = \frac{N_{agg} A_c}{2\pi r_c} \tag{9}$$

In this calculation, we have not taken into consideration the spherical end-caps. This is reasonable since the fraction of monomers that reside in the two spherical end-caps is negligible.

To find the dependence of $\bar{L}$ and $\bar{D}_H$ on the control parameters of the system (the surfactant concentration and the temperature), we recall some useful properties of threadlike micellar solutions for neutral or screened ionic surfactants. The distribution of aggregate lengths, $p(L)$, resulting from thermal equilibrium of the self-assembling threadlike micelles,[26,27] is given by

$$p(L) \propto \exp(-L/\bar{L}) \tag{10}$$

where the average micellar contour length is given by

$$\bar{L} \approx \phi^{\alpha} \exp(E_c/2k_BT) \tag{11}$$

In eq 11, ϕ is the surfactant volume fraction ($\phi \sim c$), and α is equal to 1/2.[42] It is also assumed that no rings or branches are present. E_c, the end-cap energy, is the difference in the free energy of adding surfactant molecules to the cylindrical core as compared to adding molecules to the two spherical end-caps of the micelle. The end-cap energy is assumed to be independent of concentration but is expected to increase when the spontaneous curvature, C_o, of the surfactant monolayer decreases, resulting in longer micelles.[10,38]

In the opposite case, where there are no free cylinder ends but only branching points exist, α equals $-1/2$.[11] In this case, the energy cost to form branching points, E_j, is lowered when C_o decreases because the curvature of such a junction can be lower than that of the cylindrical core.[10,38,43]

A similar analysis relates $\bar{D}_H$ to ϕ and T. If we assume that D_H is proportional to M_w^{ν} (eq 8), and since $M_w \sim \bar{L}$ for cylindrical micelles, we can show that

$$\bar{D}_H \sim \phi^{\alpha\nu} \exp(\nu E_c/2k_BT) \tag{12}$$

Results and Discussion

Cryo-TEM. Figure 2 displays cryo-TEM images of a 0.5 wt % aqueous $C_{12}E_5$ solution at three different temperatures. At 8 °C (Figure 2A), coexistence of spheroidal (arrowheads) and rather short (<50 nm) threadlike micelles (arrows) is observed. We notice the absence of short and medium length cylindrical micelles (i.e., length a few times that of the diameter of a spheroidal micelle), just as was recently found for a cationic surfactant dimer.[39] Raising the temperature to 18 °C induces micellar growth, as shown in Figure 2B. Here again, coexistence of spheroidal (arrowheads) and cylindrical micelles (arrows) is found, but the threadlike micelles are longer, typically 50 − 100 nm. The latter appear flexible and have a rather broad size distribution, in agreement with theory.[26,27] We also observe a small number of three-fold junctions or branching points (small arrow). The micelles are even longer (>100 nm) at 29 °C (Figure 2C), again with a rather broad size distribution. One can easily identify many three-fold junctions (large arrows) connecting these threadlike micelles, thus forming a network. Although much less numerous, one can find disconnected network fragments that may be related to shearing during specimen preparation (small arrow). The few four-way "crossroads" mark entanglement points or the rare four-fold junctions (arrowheads).

Next, we show the dependence of micellar growth on surfactant concentration. Figure 3 shows cryo-TEM images of three solutions at the same temperature of 18 °C, at three different concentrations. At 0.25% $C_{12}E_5$ (Figure 3A), the coexistence of spheroidal (arrowheads) and rather short (<70 nm) threadlike micelles (arrows) is observed. Again, as in Figure 2A, we do not identify short cylindrical micelles. Increasing the concentration to 0.50% (Figure 3B is the same as Figure 2B) induces micellar growth, as explained previously for Figure 2B. The micelles grow and become longer than 100 nm with a further increase in surfactant concentration to $c_c = 1.08\%$ (Figure 3C). One can easily identify many three-fold junctions (large arrows) interconnecting the cylindrical micelles, resulting in a network. The few entanglement points or rare four-fold junctions are marked by arrowheads. With raising the temperature, networks were observed for $c = c_c$ up to $T = 30$ °C (not shown), which is just below T_c, the lower critical point.

Figure 4 shows the coexisting micellar phases of a system slightly above the critical temperature we measured ($T_c = 32.6$ °C), at $T = 33.2$ °C and $c_c = 1.08$ wt %. The dark blobs (about 50 − 70 nm in size) are frost particles, occasionally seen on cryo-TEM images. In cryo-TEM micrographs of both the lower (dilute, Figure 4A) and the upper (concentrated, Figure 4B) phases, one can identify three-fold junctions (arrows) interconnecting cylindrical threads, thus forming a network. As before, we find a few disconnected network fragments. A few entanglement points or very few four-fold junctions (arrowheads) are also observed. The two networks are of equal cylinder radius, as can be observed in Figure 4, but of different junction density. At higher temperatures, where the dilute (lower) phase becomes extremely diluted, we expect the network to break into individual micelles.

Light Scattering. In Figure 5, we present data from SLS measurements performed on a solution of 0.25 wt % of $C_{12}E_5$ in water at 24 °C. Data for other solutions (0.1, 0.38, and 0.5 wt % $C_{12}E_5$) were treated in the same way. By plotting $Kc/R(q)$ versus q^2 (see eq 4), $R_{G,z}$ (= 47 nm) and the apparent M_w (= 1.39×10^6 g/mol) were extracted by linear regression. The two data points at the highest q values lie outside the range of validity of eq 4.

In Figure 6, a log−log plot of the Rayleigh ratio, $R(q)$, for $q \to 0$, $R(0)$ versus surfactant concentration (see eq 3) is plotted for different temperatures. At all temperatures, $R(0)$ increases with c; this result confirms the assumption of dilute regime conditions.[44] Notice also that $R(0)$ increases with temperature at constant surfactant concentration; this is a consequence of the micellar growth with temperature, which is reflected in the increase of the weight-average micelle molecular weight.

From DLS measurements, we were able to determine the z-average mutual translational diffusion coefficient, $\bar{D}_z$, of the particles in solution and consequently the average hydrodynamic diameter, $\bar{D}_H$ (see eq 7). A log−log plot of $\bar{D}_H$ versus apparent M_w of the micelles in 0.1, 0.25, and 0.5 wt % aqueous $C_{12}E_5$ solutions is presented in Figure 7. This linear relation indicates a power-law dependence of $\bar{D}_H \sim M_w^{\nu}$ with ν of approximately 0.6 (see Table 1). For $c = 0.25$ and 0.5 wt % $C_{12}E_5$, we find that the power-law dependence of $R_{G,z} \sim M_w^{\nu}$ also gives $\nu \sim 0.6$ (data not shown). These results indicate a similarity in the behavior of the micellar solutions and solutions of flexible polymers

(42) When rotational contribution to the entropy is taken into account, α is found to be smaller than 1/2; see McMullen, W. E.; Gelbart, W. M.; Ben-Shaul, A. *J. Phys. Chem.* **1984**, *88*, 6649.

(43) Appell, J.; Porte, G.; Berret, J. F.; Roux, D. C. *Prog. Colloid. Polymer Sci.* **1994**, *97*, 233.

(44) Buhler, E.; Munch, J. P.; Candau, S. J. *J. Phys. II* (*France*) **1995**, *5*, 765.

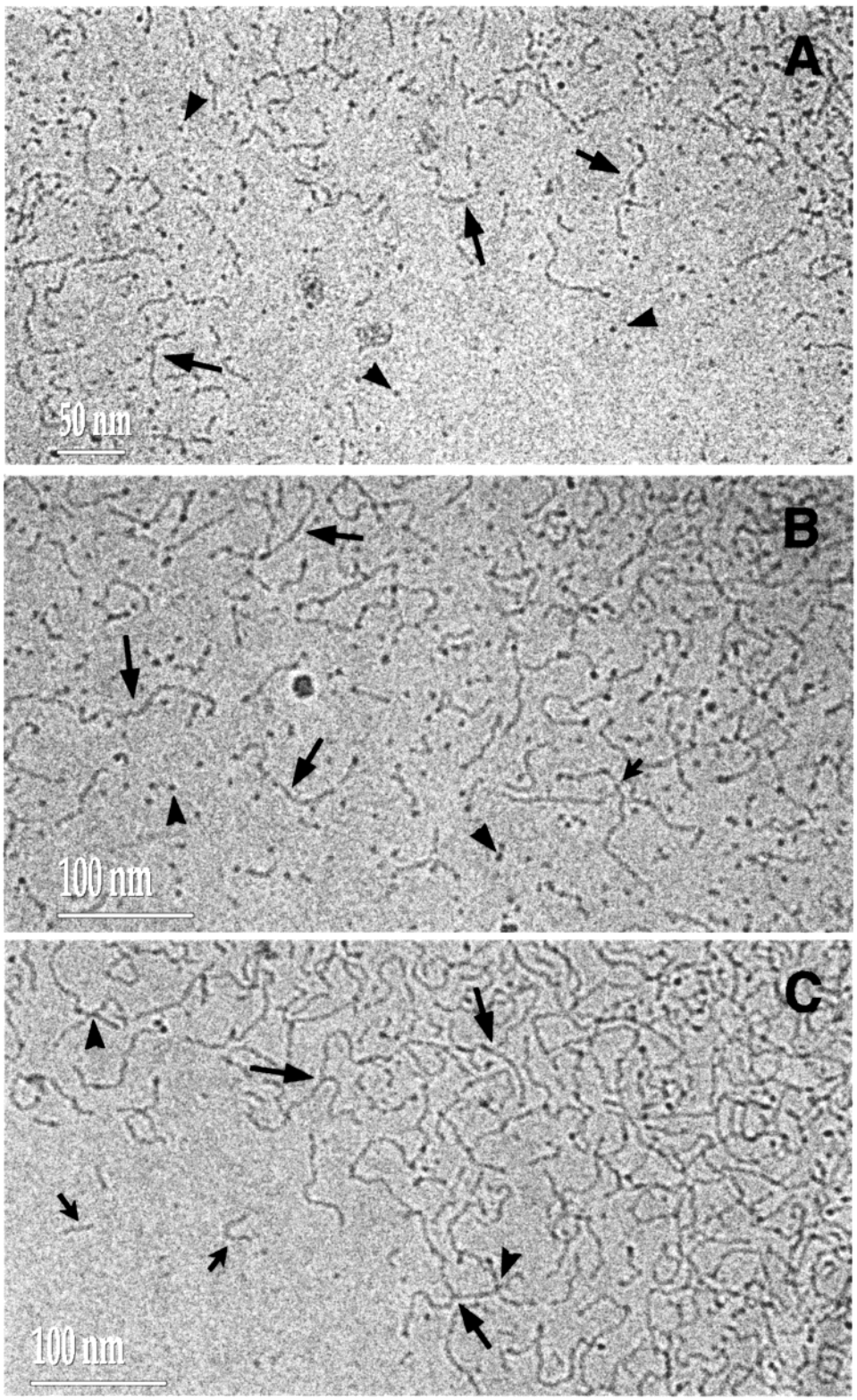

Figure 2. Cryo-TEM images of a 0.5 wt % aqueous $C_{12}E_5$ solution at three different temperatures: (A) At 8 °C, spheroidal (arrowheads) and rather short (<50 nm) threadlike micelles (arrows) coexist. (B) At 18 °C, the coexistence of spheroidal (arrowheads) and cylindrical micelles (arrows) is again identified. The threadlike micelles are typically 50 − 100 nm. Small arrow denotes three-fold junction. (C) At 29 °C, the micelles are longer (>100 nm). Large arrows mark three-fold junctions, arrowheads mark entanglement points or four-fold junctions, and small arrows mark disconnected micellar fragments.

in a good solvent (see eq 8), in agreement with a previous study on $C_{12}E_5$, conducted in semidilute conditions.[21] However, note that for $c = 0.1$ wt % (Table 1), the power ν is 0.7 ± 0.06. The reason for this behavior may be related to the fact that the micelles have some rigidity; typical persistence lengths in similar nonionic systems vary between 10 − 20 nm.[45] For a rigid rod, it was found that D_H depends on M_w^{ν} with $\nu \sim 0.85 - 1$.[46] From both SLS (N_{agg}) and cryo-TEM measurements (not shown), it ap-

(45) Magid, L. J. *J. Phys. Chem. B* **1998**, *102*, 4064 and references therein.

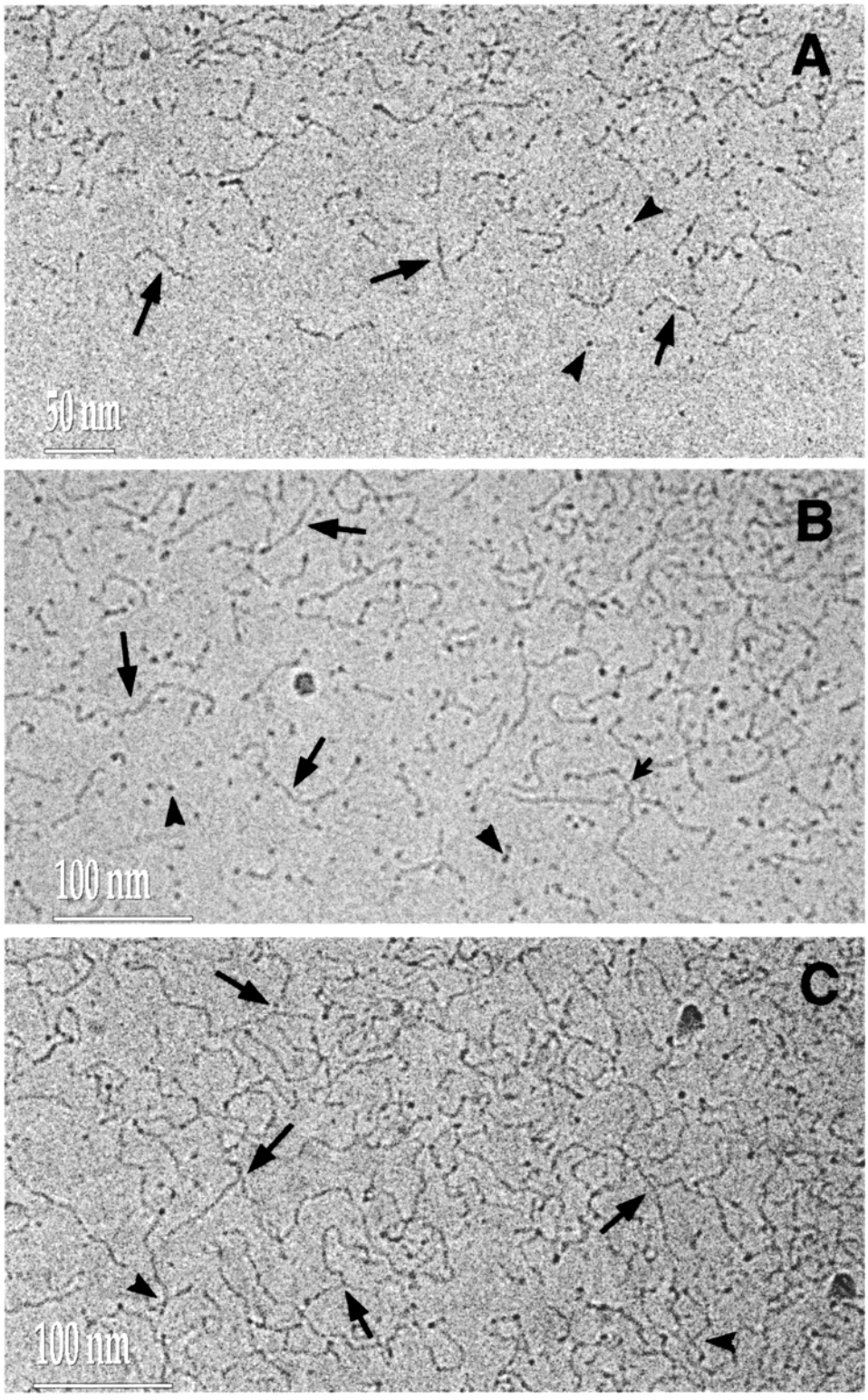

Figure 3. Cryo-TEM images of three solutions at the same temperature, 18 °C at three different concentrations: (A) at 0.25 wt % $C_{12}E_5$, the coexistence of spheroidal (arrowheads) and rather short (<70 nm) threadlike micelles (arrows) is observed. (B) At 18 °C, spheroidal (arrowheads) and cylindrical micelles (arrows) coexist (Figure 3B is the same as Figure 2B). The threadlike micelles appear flexible and are typically 50 − 100 nm. A small arrow marks a three-fold junction. (C) At $c_c = 1.08$ wt %, the micelles are longer than 100 nm. Large arrows mark three-fold junctions, and arrowheads mark entanglement points or four-fold junctions.

pears that the micelles are rather short (a few tens of nanometers) but still locally cylindrical and thus rather rigid. We explain the value of $\nu = 0.7$ as characterizing an intermediate semiflexible state between classical rigid rod and flexible chain.

We may conclude that $C_{12}E_5$ micelles in dilute aqueous solution show a uniaxial growth (cryo-TEM) with both temperature and concentration into cylindrical threads with properties similar to those of flexible polymer

(46) Harding, S. E. *Biophys. Chem.* **1995**, *55*, 69. Doi, M.; Edwards, S. F. In *The Theory of Polymer Dynamics*; Oxford University Press: Oxford, 1986.

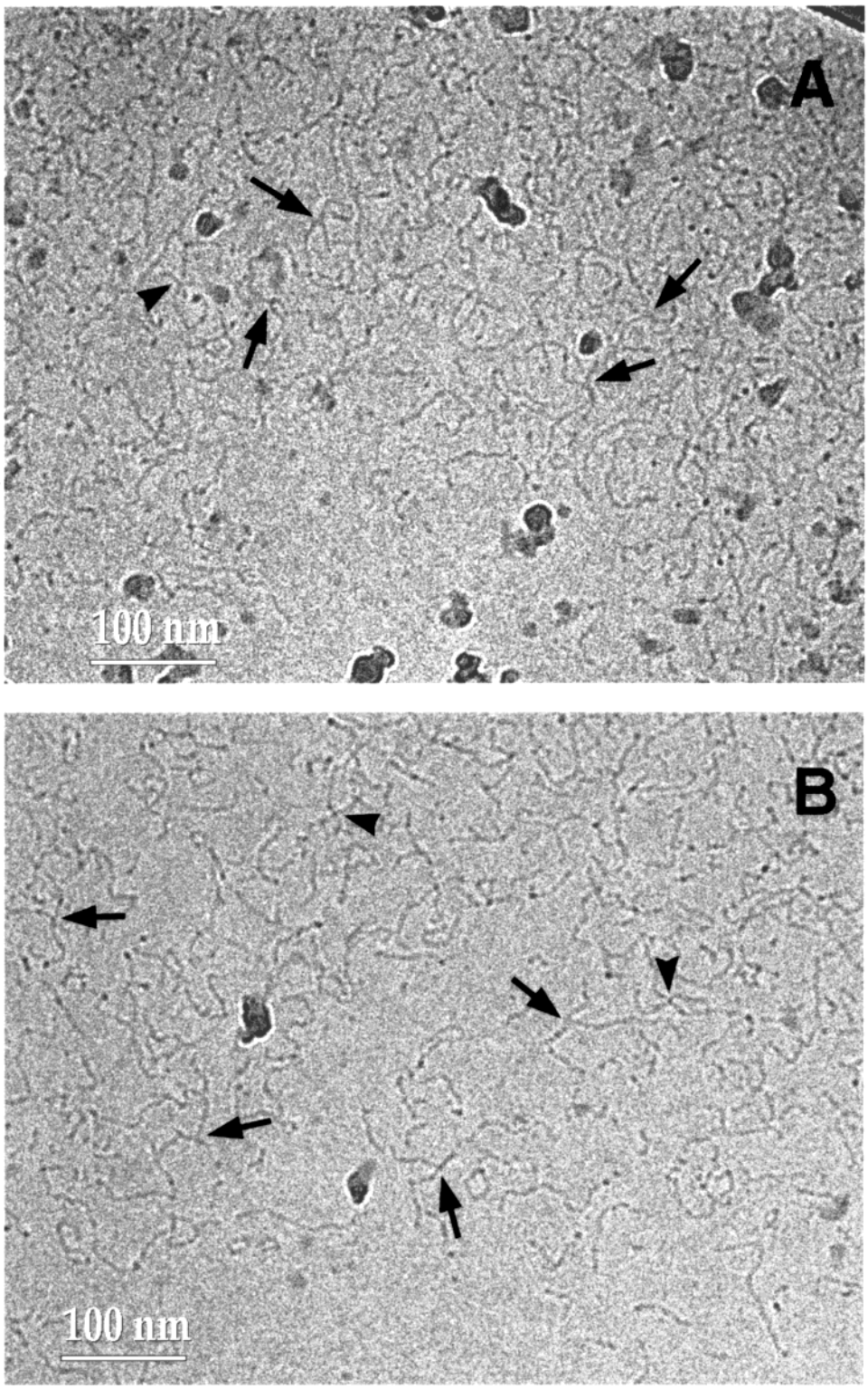

Figure 4. Cryo-TEM images of coexisting micellar networks at $T = 33.2$ °C: (A) dilute (denoted by L_1') and (B) concentrated (denoted by L_1'') phases. In both images, one can identify three-fold junctions (arrows) and four-way "crossroads" that mark entanglement points or four-fold junctions (arrowheads).

molecules (light scattering). To quantify the growth of the micelles with temperature and concentration, the average micelle contour length was calculated as described in the theoretical introduction (see eq 9). We assume that the very small minority of branched aggregates found in cryo-TEM at low temperatures and surfactant concentrations (see Figures 2A, 2B, 3A, and 3B), would not significantly influence our calculation of the mean contour lengths of micelles nor, consequently, of the end-cap energies E_c. In Figure 8A, the semilogarithmic plots of $\bar{L}$ versus the absolute temperature (K) for four solutions of $C_{12}E_5$ are found to be linear with slope "a" (values of "a" appear in Table 1). Comparing this result to eq 11 leads to the following relation between the end-cap energy, E_c, and the temperature:

$$E_c(\bar{L}) = 2aT \tag{13}$$

Table 1. Concentration Dependence of Parameters Related to the Calculation of End-Cap Energies of $C_{12}E_5$ Micelles in Water

c[g/cm^3]	ν^a	a^b [1/T]	b^c [1/T]	$E_c(\bar{L})_{T=298K}$ [k_BT]	$E_c(\bar{D}_H)_{T=298K}$ [k_BT]
0.001	0.7 ± 0.06	0.084 ± 0.004	0.083 ± 0.007	50 ± 2	53 ± 4
0.0025	0.61 ± 0.03	0.089 ± 0.003	0.093 ± 0.007	53 ± 2	56 ± 4
0.0038	0.57 ± 0.05	0.09 ± 0.01	0.095 ± 0.004	54 ± 6	57 ± 2
0.005	0.57 ± 0.05	0.088 ± 0.007	0.095 ± 0.01	52 ± 4	57 ± 7

[a] ν was found from the following relation: $\bar{D}_H \sim M_w^{\nu}$ (see Figure 7). [b] The slope "a" was found from the dependence of $\bar{L}$ on the temperature (see Figure 8A). [c] The slope "b" was found from the dependence $\bar{D}_H$ on the temperature (see Figure 8B).

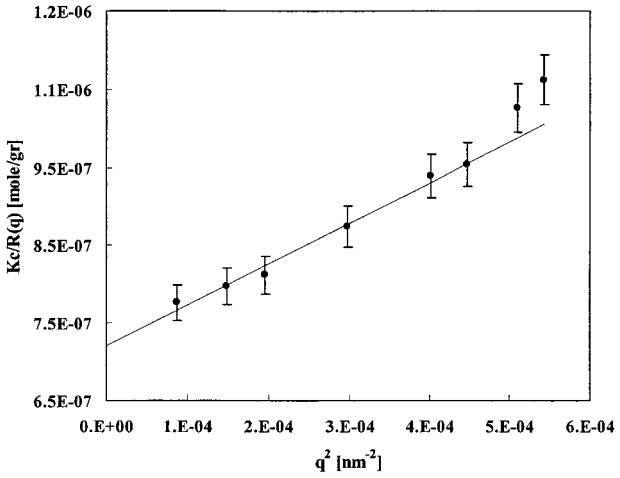

Figure 5. Plot of $Kc/R(q)$ vs q^2 for a solution of 0.25 wt % $C_{12}E_5$ in water at 24 °C. $R_{G,z}$ and the apparent M_w of the micelles are extracted from the slope and the intercept, respectively. Error bars are rms values on the basis of seven replicates.

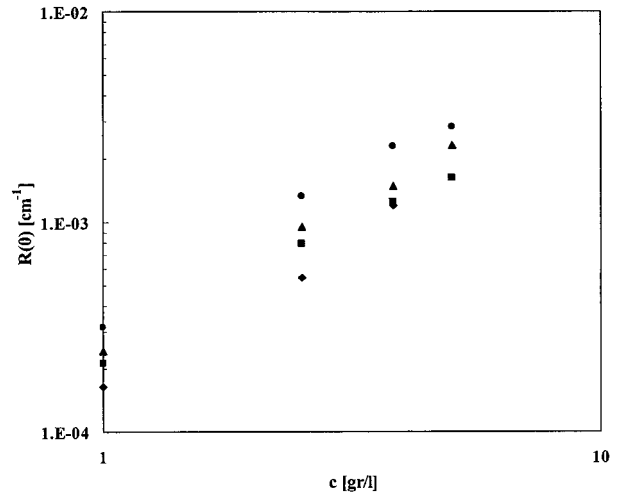

Figure 6. Concentration dependence of the Rayleigh ratio extrapolated to $q = 0$ $R(0)$, for $C_{12}E_5$ in water at $T = 15.5$ °C (◆), 18 °C (■), 20.5 °C (▲), and 24 °C (●).

where $E_c(\bar{L})$ is given in units of k_BT. Independently, we looked for the temperature dependence of $\bar{D}_H$. In Figure 8B, the semilogarithmic plot of $\bar{D}_H$ versus the absolute temperature (K) for four solutions of $C_{12}E_5$ is found to be linear, with a slope "b" (values of "b" appear in Table 1). Comparing this result to eq 12 gives a relation between the end-cap energy, E_c, and the temperature:

$$E_c(\bar{D}_H) = (2bT)/\nu \qquad (14)$$

where $E_c(\bar{D}_H)$ is given in units of k_BT. Notice that $E_c(\bar{D}_H)$ and $E_c(\bar{L})$ are approximately equal within experimental error (Table 1). The monotonic increase of $E_c(\bar{D}_H)$ and $E_c(\bar{L})$ with T is in agreement with the behavior found in the

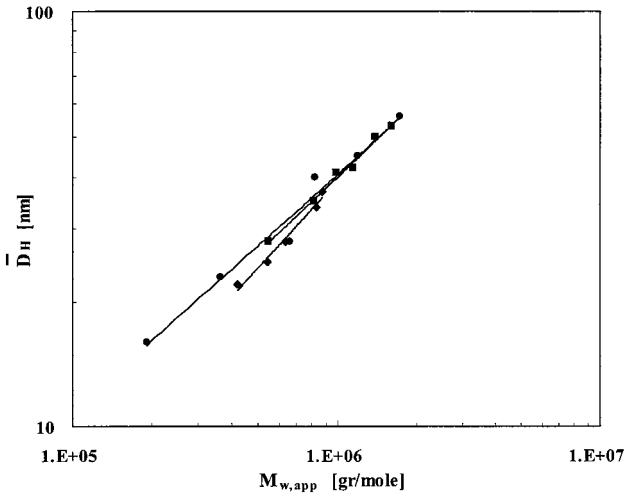

Figure 7. Dependence of the average hydrodynamic diameter $\bar{D}_H$ on the average molecular weight of the $C_{12}E_5$ micelles in water for $c = 0.1$ wt % (◆), 0.25 wt % (■), and 0.5 wt % (●). (For clarity the data points for $c = 0.38$ wt % have been omitted from the figure. These data points lie between those of $c = 0.25$ wt % and 0.5 wt %).

$C_{12}E_6$/water micellar system[3,47] and agrees qualitatively with new theoretical calculations made by Tlusty et al.[38] These results may be explained by the following arguments: the monolayer spontaneous curvature in the case of C_iE_j nonionic surfactant decreases linearly with increasing temperature.[48] By decreasing C_o, or equivalently, raising the temperature, it is less favorable for a surfactant molecule to reside in the spherical end-cap than in the cylindrical region of the micelle. The end-cap energy of the micelle represents the excess free energy for a pair of spherical end-caps relative to a threadlike region containing an equal number of surfactant molecules. In such a case, we may conclude that E_c varies with T inversely to the variation of C_o, in agreement with the experimental results. Comparison of the values of E_c for the different solutions shows that there is no dependence on the surfactant concentration (Table 1), as expected for nonionic and screened ionic surfactants.[26] Finally, we note that the values of $E_c(\bar{L})$ and $E_c(\bar{D}_H)$ (Table 1) at $T = 298$ K and 0.25% $C_{12}E_5$ are 53 ± 2 k_BT and 56 ± 4 k_BT, respectively. This corresponds to relatively large end-cap energies when compared with typical values in the literature, which range between 25 − 52 k_BT.[49−52] This high value indicates a strong tendency for micellar growth in our system.

(47) Strey, R.; Pakusch, A. *Proceeding of the Fifth International Symposium on Surfactants in Solutions*; Bordeaux, 1984; Vol. 4, p 465. Mittal, K. L., Bothorel, P., Eds.; Plenum Press: New York, 1986.
(48) Strey, R. *Colloid Polym. Sci.* **1994**, *272*, 1005.
(49) Blankschtein, D.; Thurston, G. M.; Benedek, G. B. *Phys. Rev. Lett.* **1985**, *54*, 955.
(50) Kern, F.; Lequeux, F.; Zana, R.; Candau, S. J. *Langmuir* **1994**, *10*, 1714.
(51) Hassan, P. A.; Valanlikar, B. S.; Manohar, C.; Kern, F.; Bourdieu, L.; Caudau, S. J. *Langmuir* **1996**, *12*, 4350.
(52) Candau, S. J.; Hirsch, E.; Zana, R.; Deslanti, M. *Langmuir* **1989**, *5*, 1225.

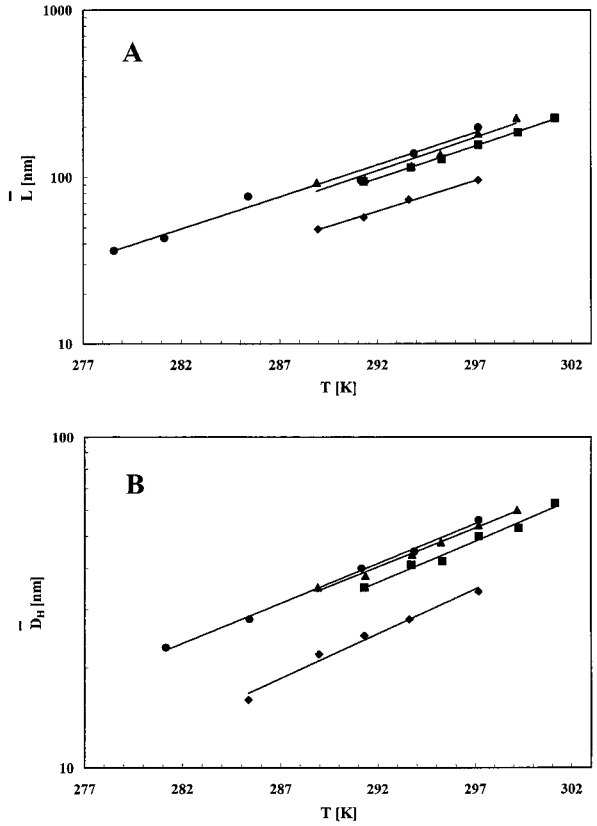

Figure 8. (A) Temperature dependence of the average micellar contour length $\bar{L}$, for $C_{12}E_5$ in water at $c = 0.1$ wt % (◆), 0.25 wt % (■), 0.38 wt % (▲), and 0.5 wt % (●). (B) Temperature dependence of the average micelle hydrodynamic diameter $\bar{D}_H$, for $C_{12}E_5$ in water at $c = 0.1$ wt % (◆), 0.25 wt % (■), 0.38 wt % (▲), and 0.5 wt % (●).

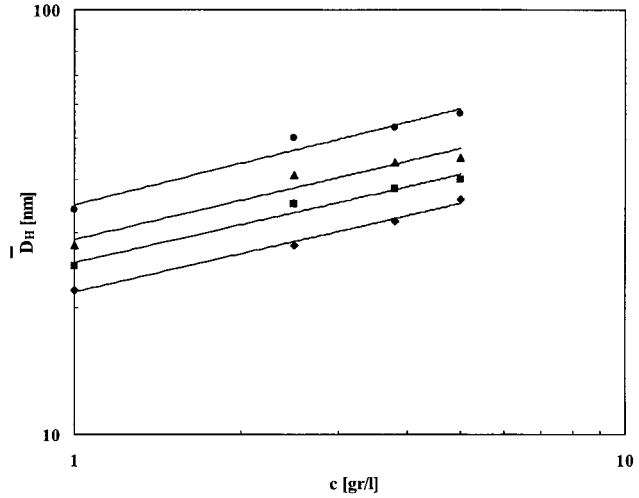

Figure 9. Concentration dependence of the average micelle hydrodynamic diameter $\bar{D}_H$, for $C_{12}E_5$ in water at $T = 15.5$ °C (◆), 18.1 °C (■), 20.5 °C (▲), and 24 °C (●).

The last point treated was the concentration dependence of $\bar{D}_H$. This dependence is characterized by a simple power-law behavior, as reflected in the linearity of the log−log plot presented in Figure 9. For all the temperatures plotted, the slope, λ, equals approximately 0.3 (Table 2). Using the value obtained independently for ν (Table 1), we find that α is equal to 0.5, in agreement with theory (eqs 11 and 12). The same value of α was found using the calculated value of $\bar{L}$ as a function of surfactant concentration (not shown here).

Table 2. Values of λ, Obtained from the Dependence of $\bar{D}_H$ on Surfactant Concentration, at Four Different Temperatures

T (°C)	λ^a
15.5	0.3 ± 0.1
18.1	0.3 ± 0.03
20.5	0.31 ± 0.05
24	0.32 ± 0.04

[a] λ was found from the dependent $\bar{D}_H$ on surfactant concentration (see Figure 9).

Conclusions

In this work we have used cryo-TEM and light scattering to study the micellar growth and network formation in aqueous solutions of the nonionic surfactant $C_{12}E_5$. The present work shows by cryo-TEM the gradual formation of micellar networks from disconnected polymer-like micelles as temperature is raised. The direct structural observation by cryo-TEM substantiates the relation between criticality of binary systems and the existence of micellar networks.

At very low temperatures and surfactant concentrations, well below the critical point, we have observed the coexistence of short disconnected cylindrical and spherical micelles. With increasing temperature and concentration, we have identified uniaxial micellar growth into threadlike objects having properties resembling those of flexible polymers in a good solvent ($\nu \sim 0.6$). Static and dynamic light scattering show that the mean micelle contour length $\bar{L}$ increases as $c^{0.5}$, in agreement with theory.[26,27] We suggest that the effect of temperature on micellar growth can be explained through its effect on E_c, the end-cap energy of the micelles. We find E_c to be linearly dependent on temperature. This is in qualitative agreement with recent calculations of Tlusty et al.[38] and with the behavior found in the $C_{12}E_6$/water micellar system.[3,47] It was experimentally shown that the spontaneous curvature, C_o, of C_iE_j surfactant monolayers decreases linearly with increasing temperature.[48] Consequently, the energy penalty for a surfactant molecule to reside in the spherical end-cap in comparison to the cylindrical core, as is reflected in E_c, should increase when the spontaneous curvature of the surfactant monolayer decreases. As the temperature is further increased, we observe branch formation.

The phenomenon of branching is observed in $C_{12}E_5$ micelles, except at the very lowest concentrations and temperatures. The tendency of the surfactant molecules to form branched micelles increases markedly as the critical point and two-phase separation curve is approached because the energy cost to form end-caps in contrast to branches increases with temperature. We have clearly identified the existence of a network topology in this region of the phase diagram. Moreover, we have shown that at a temperature slightly above the critical point, the two coexisting, concentrated and dilute, phases are of a network topology. This supports the theoretical suggestion that the same physics of entropic interactions within semiflexible networks that govern swollen microemulsions could also explain the criticality and phase behavior of certain binary micellar solutions.[7]

Consistent with theory,[11,12,53] we found that the formation of those networks is not only temperature dependent, but also concentration dependent. At $T = 18$ °C, we observed a transition from threadlike micelles ($c = 0.25\%$, see Figure 3A) to individual branched micelles ($c = 0.5\%$, see Figure 3B), to a network of branched cylindrical

(53) Tlusty, T.; Safran, S. A.; Strey, R. *Phys. Rev. Lett.* **2000**, *84*, 1224.

micelles ($c = 1.08\%$, see Figure 3C). We have also shown that branched cylindrical networks appear already at $c = 0.5\%$ for a temperature of $T = 29$ °C (see Figure 2C), indicating that junctions at this temperature are energetically much more favorable than end-caps. However, at a very low temperature of $T = 2$ °C we observed only the coexistence of spheroidal and threadlike micelles, even at a concentration of $c = 1.5\%$ (not shown). This in turn shows that end-caps are energetically much more favorable than junctions at $T = 2$ °C. Assuming that the junctions and end-caps energies, E_j and E_c, respectively, depend linearly but inversely on temperature,[38] we conclude that junctions are somewhat more energetically favorable than end-caps at $T = 18$ °C. According to theory,[53] the transition from unbranched to branched micelles depends on the difference between the junction and end-cap energies: the more favorable E_j is over E_c, (i.e., the higher the temperature for nonionic surfactants), the lower the surfactant concentration at which this transition occurs. Indeed, interconnected cylindrical micelles start to appear at lower temperatures as surfactant concentration increases.

Acknowledgment. We thank S. A. Safran and T. Tlusty for useful discussions. We also thank S. A. Safran for critical reading of the manuscript. We thank the reviewers for most useful comments. This work was supported in part by a “Center of Excellence” grant from the Israel Science Foundation founded by the Israel Academy of Sciences and Humanities.

LA991231Q